Inorg. Chem. **2008**, *47*, 2543−2551

Structural, Photophysical, and Catalytic Properties of Au(I) Complexes with 4-Substituted Pyridines

J. C. Y. Lin,[†] S. S. Tang,[‡] C. Sekhar Vasam,[†] W. C. You,[‡] T. W. Ho,[†] C. H. Huang,[†] B. J. Sun,[†] C. Y. Huang,[†] C. S. Lee,[†] W. S. Hwang,[†] A. H. H. Chang,*[,†] and Ivan J. B. Lin*[,†]

Department of Chemistry, National Dong Hwa University, Hualien, Taiwan, 97401, and Department of Chemistry, Fu Jen Catholic University, Taipei, Taiwan, 24205

Received September 21, 2007

Ionic gold(I) complexes with general formula of $[Au(Py)_2][AuCl_2]$ and $[Au(Py)_2][PF_6]$ (Py = 4-substituted pyridines) have been synthesized. Structures of five Au(I) complexes and a Ag(I) complex were determined by single crystal X-ray diffraction. Evidence for cationic aggregation of $[Au(py)_2][PF_6]$ complexes in solution was obtained by conductivity measurements and by the isosbestic point observed from variable temperature UV–visible absorption spectra. All compounds were luminous in the solid state. Calculations employing density functional theory were performed to shed light on the nature of the electronic transitions. While the $[Au(4\text{-dmapy})_2][AuCl_2]$ (4-dmapy = 4-dimethylaminopyridine) and $[Au(4\text{-pic})_2][AuCl_2]$ (4-pic = 4-picoline) emissions were found to be mainly ligand in nature, their $[PF_6]^-$ counterparts involved a Au···Au-interaction imbedded in the highest occupied molecular orbital. $[Au(4\text{-dmapy})_2][AuCl_2]$ was found to be an efficient catalyst for Suzuki cross-coupling of aryl bromide and phenylboronic acid.

Introduction

The significance of Au(I) complexes is manifested in several fascinating properties, among which the aurophilic attractions and photophysical properties have been intensively studied.[1] Aurophilicity, often attributed to relativistic effects, is an attraction between the Au(I) ions with their closed d^{10} shell.[2] Because of a similarity in magnitude with hydrogen bonding, it could play a key role in molecular aggregation in both solid state and solution. While the role of aurophilicity in the solid-state aggregations is well established, less has been studied in solution.[3] Aurophilic interaction is also known to contribute to the intriguing luminescent behavior of Au(I) complexes.[4] Yet, its nature has not been completely understood.

* To whom correspondence should be addressed. E-mail: ijblin@mail.ndhu.edu.tw (I.J.B.L), hhchang@mail.ndhu.edu.tw (A.H.H.C.). Tel: 886-3-863-3599. Fax: 886-3-863-3570.

† National Dong Hwa University.

‡ Fu Jen Catholic University.

(1) (a) Schmidbaur, H. *Nature* **2001**, *413*, 31. (b) Zhang, H. X.; Che, C. M. *Chem.—Eur. J.* **2001**, *7*, 4887. (c) Hayashi, A.; Olmstead, M. M.; Attar, S.; Balch, A. L. *J. Am. Chem. Soc.* **2002**, *124*, 5791. (d) Yip, S. K.; Cheng, E. C. C.; Yuan, L. H.; Zhu, N.; Yam, V. W. W. *Angew. Chem., Int. Ed.* **2004**, *43*, 4954. (e) McArdle, C. P.; Irwin, M. J.; Jennings, M. C.; Vittal, J. J.; Puddephatt, R. J. *Chem.—Eur. J.* **2002**, *8*, 723. (f) Barnard, P. J.; Wedlock, L. E.; Baker, M. V.; Berners-Price, S. J.; Joyce, D. A.; Skelton, B. W.; Steer, J. H. *Angew. Chem., Int. Ed.* **2006**, *45*, 5966. (g) Lee, Y.; Eisenberg, R. *J. Am. Chem. Soc.* **2003**, *125*, 7778. (h) Bardaji, M.; Jones, P. G.; Laguna, A.; Villacampa, M. D.; Villaverde, N. *Dalton Trans.* **2003**, 4529. (i) Chen, J. H.; Mohamed, A. A.; Abdou, H. E.; Bauer, J. A. K.; Fackler, J. P.; Bruce, A. E.; Bruce, M. R. M. *Chem. Commun.* **2005**, 1575. (j) Bachman, R. E.; Bodolosky-Bettis, S. A.; Glennon, S. C.; Sirchio, S. A. *J. Am. Chem. Soc.* **2000**, *122*, 7146. (k) Kui, S. C. F.; Huang, J. S.; Sun, R. W. Y.; Zhu, N. Y.; Che, C. M. *Angew Chem., Int. Ed.* **2006**, *45*, 4663. (l) Wang, H. M. J.; Vasam, C. S.; Tsai, T. Y. R.; Chen, S.-H.; Chang, A. H. H.; Lin, I. J. B. *Organometallics,* **2005**, *24*, 486–493. (m) Habermehl, N. C.; Eisler, D. J.; Kirby, C. W.; Yue, N. L. S.; Puddephatt, R. J. *Organometallics* **2006**, *25*, 2921.

(2) (a) Pyykko, P. *Angew. Chem., Int. Ed.* **2004**, *43*, 4412. (b) Pyykko, P. *Chem. Rev.* **1997**, *97*, 597. (c) Schmidbaur, H. *Gold Bull.* **2000**, *33*, 3. (d) Brandys, M. C.; Puddephatt, R. J. *Chem. Commun.* **2001**, 1280.

(3) (a) Deak, A.; Megyes, T.; Tarkanyi, G.; Kiraly, P.; Biczok, L.; Palinkas, G.; Stang, P. J. *J. Am. Chem. Soc.* **2006**, *128*, 12668. (b) Yu, S.-Y.; Zhang, Z.-X.; Cheng, E. C. C.; Li, Y. Z.; Yam, V. W. W.; Huang, H. P.; Zhang, R. *J. Am. Chem. Soc.* **2005**, *127*, 17994. (c) de la Riva, H.; Pintado-Alba, A.; Nieuwenhuyzen, M.; Hardacre, C.; Lagunas, M. C. *Chem. Commun.* **2005**, 4970. (d) Stott, T. L.; Wolf, M. O.; Patrick, B. O. *Inorg. Chem.* **2005**, *44*, 620. (e) Zank, J.; Schier, A.; Schmidbaur, H. *Dalton Trans.* **1998**, 323. (f) Tang, S. S.; Chang, C. P.; Lin, I. J. B.; Liou, L. S.; Wang, J. C. *Inorg. Chem.* **1997**, *36*, 2294. (g) Feng, D. F.; Tang, S. S.; Liu, C. W.; Lin, I. J. B.; Wen, Y.-S.; Liu, L.-K. *Organometallics* **1997**, *16*, 901.

(4) (a) Rawashdeh-Omary, M. A.; Omary, M. A.; Patterson, H. H.; Fackler, J. P. *J. Am. Chem. Soc.* **2001**, *123*, 11237. (b) Fu, W. F.; Chan, K. C.; Miskowski, V. M.; Che, C. M. *Angew Chem., Int. Ed.* **1999**, *38*, 2783. (c) Yam, V. W. W.; Chan, C. L.; Li, C. K.; Wong, K. M. C. *Coord. Chem. Rev.* **2001**, *216*, 173. (d) White-Morris, R. L.; Olmstead, M. M.; Balch, A. L. *J. Am. Chem. Soc.* **2003**, *125*, 1033. (e) Coker, N. L.; Krause Bauer, J. A.; Elder, R. C. *J. Am. Chem. Soc.* **2004**, *126*, 12.

10.1021/ic701872f CCC: $40.75
Published on Web 03/05/2008

Au(I) complexes with ligands of phosphines and thiolates have been the topic of many investigations; complexes of nitrogen donor pyridine (Py) ligands have been less scrutinized,[5] owing to perhaps their thermal/photo instability. Nevertheless, there are several known applications, for example, the antiarthritic activity of Au(I)−Py complexes[6] and the use of pyridine ligands to facilitate the extraction of gold in mining.[7] Recently, Au(I)−Py compounds have been considered as an emerging class of luminescent materials,[5i,j] and utilized as catalysts in olefin aziridination,[5k] carbene insertion into benzene,[5k] cycloisomerization of β-hydroxyallenes,[5g] and alcohol oxidation.[5h]

In this work, Au(I) complexes with four 4-substituted pyridines were synthesized; their solid state supramolecular structures, solution aggregation behavior, and photophysical properties were examined. Density functional theory (DFT) calculations were performed to shed light on the nature of bonding and of electronic transitions. As far as we know, only one similar study on Au−Py complexes has appeared recently.[5j] This investigation certainly highlights the role of aurophilicity in the stability and reactivities of Au(I)−Py compounds. In view of the "gold rush" in various branches of modern science,[8] we also report the utilization of a Au(I)−Py complex as catalyst for the Suzuki cross-coupling reaction. The abbreviations for the Py ligands and Au(I)−Py complexes are given in Scheme 1.

Scheme 1. Au(I) Complexes with Different Substituted Pyridines

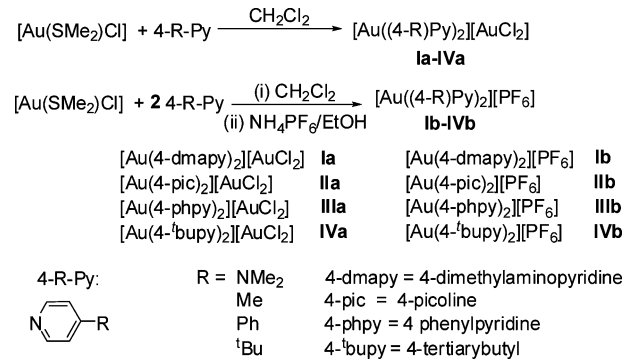

Experimental Section

General Information. Elemental analysis was carried out at the Taiwan Instrumentation Center. ^{1}H NMR spectra were recorded on a Bruker AC-F300 spectrometer; UV–vis spectra were obtained on a Shimadzu UV-2101PC spectrophotometer. Emission, excitation, and lifetime spectra were acquired on an Aminco Bowman AD2 luminescent spectrofluorometer.

Single crystal X-ray data of $[Au(4\text{-dmapy})_2][AuCl_2]$, $[Au(4\text{-dmapy})_2][PF_6]$ and $[Au(4\text{-phpy})_2][PF_6]$ were collected on a Bruker SMART APEX diffractometer, and those of $[Au(4\text{-pic})_2][AuCl_2]$ and $[Au(4\text{-pic})_2][PF_6]$ on a Siemens P4 diffractometer. All the structures were solved and refined by employing SHELXL 97; non hydrogen atoms were refined anisotropically. Hydrogen atoms were placed in calculated positions. The crystal data and experimental details are given in the Supporting Information Table S1.

Theoretical Method. The calculations of density functional B3LYP[9a,b] with LanL2DZ[9c] basis sets were carried out for free 4-dmapy and ion-pairs, $[Au(4\text{-dmapy})_2][AuCl_2]$ and $[Au(4\text{-pic})_2][AuCl_2]$, mononuclear $[Au(4\text{-dmapy})_2]^+$, $[Au(4\text{-pic})_2]^+$, and $AuCl_2^-$, and dinuclear $[(Au(4\text{-dmapy})_2)_2]^{2+}$ and $[(Au(4\text{-pic})_2)_2]^{2+}$. Note that with basis set LanL2DZ, the ab initio effective core potentials were employed to replace the core electrons of Au, in which mass-velocity and Darwin relativistic effects have been incorporated. The Gaussian 98 program[10] was utilized in the ab initio electronic structure calculations.

$[Au(4\text{-dmapy})_2][AuCl_2]$ (Ia). 4-dmapy (125 mg, 1.02 mmol) was added to a dichloromethane solution (10 mL) of $Au(SMe_2)Cl$ (300 mg, 1.02 mmol) and was stirred for 2 h at room temperature in the dark. After removing the solvent under vacuum, the residue was washed with ether to give a light yellow crude product. Recrystallization by slow diffusion of ether into the CH_3CN solution produced light yellow crystals of $[Au(4\text{-dmapy})_2][AuCl_2]$. Yield: 85%. Mp: 142 °C. Anal. Calcd. for $C_{14}H_{20}N_4Au_2Cl_2$: C = 23.71; H = 2.84; N = 7.90. Found: C = 23.69; H = 2.83; N = 7.66. FAB/MS: 441.2 m/z = $[Au(4\text{-dmapy})_2]^+$. ^{1}H NMR (DMSO-d_6): 8.20 (d, 4H, J = 7.2 Hz, o-H of py); 6.81 (d, 4H, J = 7.4 Hz, m-H of py); 3.07 ppm (s, 12H, $N(CH_3)_2$).

Complexes **IIa-IVa** were similarly prepared. Data for each complex are given below.

$[Au(4\text{-pic})_2][AuCl_2]$ (IIa). Yield: 65%. Mp: 130 °C. Anal. Calcd. for $C_{12}H_{14}N_2Au_2Cl_2$: C = 22.14; H = 2.17; N = 4.30. Found: C = 22.06; H = 2.20; N = 4.09. FAB/MS: 383 m/z = $[Au(4\text{-pic})_2]^+$. ^{1}H NMR (DMSO-d_6): 8.72 (d, 4H, J = 6.1 Hz, o-H of py); 7.66 (d, 4H, J = 5.6 Hz, m-H of py); 2.40 ppm (s, 6H, CH_3).

$[Au(4\text{-phpy})_2][AuCl_2]$ (IIIa). Yield: 55%. Mp: 131 °C. Anal. Calcd. for $C_{22}H_{18}N_2Au_2Cl_2$: C = 34.09; H = 2.34; N = 3.61. Found: C = 33.99; H = 2.32; N = 3.65. FAB/MS: 507.2 m/z = [Au(4-

(5) (a) Yip, J. H. K.; Feng, R.; Vittal, J. J. *Inorg. Chem.* **1999**, *38*, 3586. (b) Adam, H. N.; Hiller, W.; Strahle, J. *Z. Anorg. Allg. Chem.* **1982**, *485*, 81. (c) Conzelmann, W.; Hiller, W.; Strahle, J.; Sheldrick, G. M. *Z. Anorg. Allg. Chem.* **1984**, *512*, 169. (d) Jones, P. G.; Ahrens, B. *Z. Naturforsch.* **1998**, *B53*, 653. (e) Freytag, M.; Jones, P. G. *Chem. Commun.* **2000**, 277. (f) Ray, P. C.; Sen, D. S. *J. Indian Chem. Soc.* **1930**, *6*, 67. (g) Li, Z.; Ding, X.; He, C. *J. Org. Chem.* **2006**, *71*, 5876. (h) Guan, B.; Xing, D.; Cai, G.; Wan, X.; Yu, N.; Fang, Z.; Yang, L.; Shi, Z. *J. Am. Chem. Soc.* **2005**, *127*, 18004. (i) Kim, P.-S. G.; Hu, Y.; Brandys, M.-C.; Burchell, T. J.; Puddephatt, R. J.; Sham, T. K. *Inorg. Chem.* **2007**, *46*, 949. (j) Fernández, E. J.; Laguna, A.; López-de-Luzuriaga, J. M.; Monge, M.; Montiel, M.; Olmos, M. E.; Pérez, J.; Rodríguez-Castillo, M. *Gold Bull.* **2007**, *40*, 172. (k) Li, Z.; Ding, X.; He, C. *J. Org. Chem.* **2006**, *71*, 5876. (l) Hill, D. T. U.S. Patent 4098887, **1978**. (m) Kristjansdottir, S. S.; Thompson, J. S. U.S. Patent 5484470, **1996**. (n) Catalano, V. J.; Malwitz, M. A.; Etogo, A. O. *Inorg. Chem.* **2004**, *43*, 5714–5724. (o) Catalano, V. J.; Moore, A. L. *Inorg. Chem.* **2005**, *44*, 6558–6566. (p) Catalano, V. J.; Etogo, A. O. *Inorg. Chem.* **2007**, *46*, 5608–5615. (q) Bayler, A.; Schmidbaur, H. *J. Am. Chem. Soc.* **1996**, *118*, 5324. (r) Pyykkö, P.; Schneider, W.; Bauer, A.; Bayler, A.; Schmidbaur, H. *Chem. Commun.* **1997**, 1111.

(6) (a) Rhodes, M. D.; Sandler, P. J.; Scawen, M. D.; Silver, S. *J. Inorg. Biochem.* **1992**, *46*, 129. (b) de Fremont, P.; Stevens, E. D.; Eelman, M. D.; Fogg, D. E.; Nolan, S. P. *Organometallics* **2006**, *25*, 5824.

(7) (a) Akimbaeva, A. M.; Ergozhin, E. E. *Russ. J. Appl. Chem.* **2004**, *77*, 1754. (b) Räisänen, M. T.; Kemell, M.; Leskelä, M.; Repo, T. *Inorg. Chem.* **2007**, *46*, 3251.

(8) (a) Hashmi, A. S. K.; Hutchings, G. J. *Angew. Chem., Int. Ed.* **2006**, *45*, 7896. (b) Astruc, D.; Lu, F.; Aranzaes, J. R. *Angew. Chem., Int. Ed.* **2005**, *44*, 7852. (c) Jaramillo, T. F.; Baeck, S. H.; Cuenya, B. R.; McFarland, E. W. *J. Am. Chem. Soc.* **2003**, *125*, 7148. (d) Pradhan, N.; Pal, A.; Pal, T. *Langmuir* **2001**, *17*, 1800. (e) Chen, M. S.; Goodman, D. W. *Acc. Chem. Res.* **2006**, *39*, 739. (f) McKeage, M. J.; Maharaj, L.; Berners-Price, S. J. *Coord. Chem. Rev.* **2002**, *232*, 127. (g) Jones, V. C. J.; Taube, D.; Ziatdinov, V. R.; Periana, R. A.; Nielsen, R. J.; Oxgaard, J.; Goddard III, W. A. *Angew. Chem., Int. Ed.* **2004**, *43*, 4626.

(9) (a) Becke, A. D. *J. Chem. Phys.* **1993**, *98*, 5648. (b) Lee, C.; Yang, W.; Parr, R. G. *Phys. Rev. B* **1988**, *37*, 785. (c) Hay, P. J.; Wadt, W. R. *J. Chem. Phys.* **1985**, *82*, 299.

(10) Frisch, M. J. et al. *GAUSSIAN 98*, Revision A.5; Gaussian, Inc.: Pittsburgh, PA, 1998.

phpy)$_2$]$^+$. ^{1}H NMR (DMSO-d_6): 8.62 (d, 4H, J = 6.0 Hz, *o*-H of py); 7.80 (d, 4H, J = 6.9 Hz, *m*-H of py); 7.72–7.47 ppm (m, 10H, Ph).

[Au(4-*t*-butylpy)$_2$][AuCl$_2$] (IVa). Yield: 58%. Mp: 142 °C. Anal. Calcd. for $C_{18}H_{26}N_2Au_2Cl_2$: C = 29.40; H = 3.56; N = 3.81. Found: C = 29.57; H = 3.65; N = 3.73. FAB/MS: 467 m/z = [Au(4-^{t}butylpy)$_2$]$^+$. ^{1}H NMR($CDCl_3$): 8.77 (d, 4H, J = 7.0 Hz, *o*-H of py); 7.50 (d, 4H, J = 6.8 Hz, *m*-H of py); 1.36 ppm (s, 18H, $C(CH_3)_3$).

[Au(4-dmapy)$_2$][PF$_6$] (Ib). 4-dmapy (250 mg, 2.04 mmol) was added to a dichloromethane solution (10 mL) of Au(SMe_2)Cl (300 mg, 1.02 mmol), followed by a EtOH (5 mL) solution of NH_4PF_6 (166 mg, 1.02 mmol) in the dark. The resultant solution was stirred for 2 h at room temperature. The solvent was then removed under vacuum to give a light yellow residue, which was washed with CH_3CN/ether and recrystallized from CH_3CN/EtOH. Yield: 91%. Mp: 181 °C. Anal. Calcd. for $C_{14}H_{20}N_4AuPF_6$: C = 28.68; H = 3.44; N = 9.56. Found: C = 29.09; H = 3.52; N = 10.01. FAB/MS: 441.2 m/z = [Au(4-dmapy)$_2$]$^+$. ^{1}H NMR (DMSO-d_6): 8.20 (d, 4H, J = 7.3 Hz, *o*-H of py); 6.81 (d, 4H, J = 7.4 Hz, *m*-H of py); 3.07 ppm (s, 12H, $N(CH_3)_2$).

Compounds **IIb**-**IVb** were prepared in the same manner as **Ib**. Data for **IIb**-**IVb** are given below.

[Au(4-pic)$_2$][PF$_6$] (IIb). Yield: 87%. Mp: 139 °C (dec without melting). Anal. Calcd. for $C_{12}H_{14}N_2AuPF_6$: C = 27.29; H = 2.61; N = 5.30. Found: C = 27.49; H = 2.60; N = 5.17. FAB/MS: 383 m/z = [Au(4-pic)$_2$]$^+$. ^{1}H NMR (DMSO-d_6): 8.72 (d, 4H, J = 5.5 Hz, *o*-H of py); 7.66 (d, 4H, J = 4.9 Hz, *m*-H of py); 2.40 ppm (s, 6H, CH_3).

[Au(4-phpy)$_2$][PF$_6$] (IIIb). Yield: 84%. Mp: 174 °C. Anal. Calcd. for $C_{22}H_{18}N_2AuPF_6$: C = 40.51; H = 2.78; N = 4.29. Found: C = 40.51; H = 2.84; N = 4.12. FAB/MS: 507.2 m/z = [Au(4-phpy)$_2$]$^+$. ^{1}H NMR (DMSO-d_6): 8.94 (d, 4H, J = 6.1 Hz, *o*-H of py); 8.20 (d, 4H, J = 6.4 Hz, *m*-H of py); 7.98–7.53 ppm (m, 10H, Ph).

[Au(4-*t*-butylpy)$_2$][PF$_6$] (IVb). Yield: 81%. Mp: 150 °C. Anal. Calcd. for $C_{18}H_{26}N_2AuPF_6$: C = 35.31; H = 4.28; N = 4.57. Found: C = 35.25; H = 4.30; N = 4.74. FAB/MS: 467 m/z = [Au(4-^{t}butylpy)$_2$]$^+$. ^{1}H NMR (DMSO-d_6): 8.77 (d, 4H, J = 6.6 Hz, *o*-H of py); 7.74 (d, 4H, J = 6.7 Hz, *m*-H of py); 1.32 ppm (s, 18H, $C(CH_3)_3$).

General Procedure for the Suzuki Cross-Coupling Reaction. Phenylboronic acid (90 mg, 0.70 mmol), *p*-bromotoluene (100 mg, 0.58 mmol), [Au(4-dmapy)$_2$][$AuCl_2$] (21 mg, 0.03 mmol), and K_2CO_3 (120 mg, 0.87 mmol) were mixed in dimethylformamide (DMF, 1 mL). Reactions were carried out at both 130 and 25 °C under both aerobic and N_2 atmospheric conditions. Yields and conversions were determined by gas chromatography (GC) analysis.

Results and Discussion

Complexes of **Ia**−**IVa** were obtained by the reaction of one equivalent of Au(SMe_2)Cl in CH_2Cl_2 with one equivalent of 4-dampy, 4-pic, 4-phpy and 4-^{t}bupy, respectively, followed by recrystallization from CH_3CN/Et_2O. On the other hand, **Ib**−**IVb** were prepared by the reaction of pyridines with Au(SMe_2)Cl in 2:1 molar ratios in CH_2Cl_2 followed by the addition of 1 molar of NH_4PF_6 in EtOH. Complexes **I**−**IV** were moderately stable in the solid state.

The complexes were characterized by elemental analyses, conductivity measurements, ^{1}H NMR, FAB Mass, and electronic spectroscopies. In particular, five Au(I)−Py complexes, **Ia**, **Ib**, **IIa**, **IIb**, and **IIIb**, were examined by X-ray crystallography.

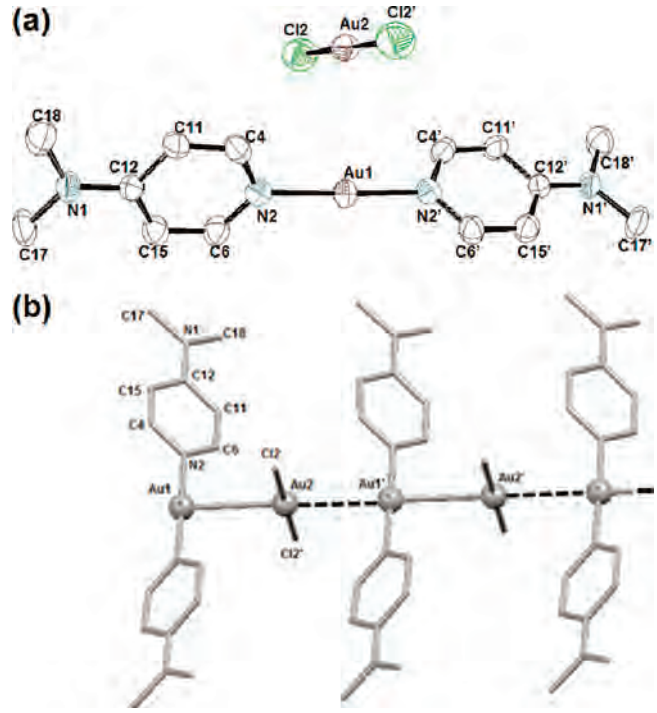

Figure 1. (a) ORTEP diagram of **Ia** (50% probability ellipsoids), (b) crystal packing diagram of **Ia** with a [+ − + − ···] pattern (the hydrogen atoms have been omitted for clarity). Selected bond lengths (Å) and angles (deg): Au(1)−Au(2), 3.2005(5); Au(1)−N(2), 2.022(3); N(2)−C(6), 1.345(5); N(2)−C(4), 1.348(6); N(1)−C(12), 1.357(5); Au(2)−Cl(2), 2.2659(16); N(2)−Au(1)−(N2′), 177.7(2); C(4)−N(2)−C(6), 116.3(4); Cl(2)−Au(2)−Cl(2′), 179.73(7). Au(1)−Au(2)−Au(1), 180.0.

Crystal Structures. [Au(4-dmapy)$_2$][AuCl$_2$] Ia. As seen in Figure 1, compound **Ia** forms an ion-pair (+ −), comprising a linear [Au(4-dampy)$_2$]$^+$ cation and a linear [$AuCl_2$]$^-$ anion with normal Au−N and Au−Cl bond lengths (Figure 1caption).[5a–e] The two pyridyl rings are twisted by about 79°. The short C(12)−N(1) distance (ca. 1.36 Å) is consistent with the delocalization of the amine lone pair together with the electrons of the pyridine ring.[11] The cation and anion are associated perpendicularly through a Au···Au contact of about 3.20 Å.[1] Neighboring ion-pairs are further linked through a Au···Au contact of about 3.27 Å to generate a linear polymer with alternating cations and anions. The similar [+ − + − ···] packing pattern has been previously reported.[5c,g,r] The discrete trinuclear {[AuL_2]$^+$-[LAuCl][$AuCl_2$]$^-$} (L = 2-aminopyridine),[5a] and tetranuclear {[AuX_2][AuL_2]$_2$[AuX_2]} (L = unsubstituted pyridine, X = Cl, Br, I; L = 3-bromopyridine, X = Cl) compounds[5b,c] are also known. Secondary interactions of C−H···Cl, C−H···Au, and C−H···π are responsible for holding the polynuclear chains in adjacent positions in the supramolecular assembly (see Supporting Information) as observed by other researchers.[12]

[Au(4-dmapy)$_2$][PF$_6$] Ib. The molecular cations of **Ib** have linearly coordinated Au(I) centers with essentially coplanar pyridines (Figure 2). The cations are packed in [+

(11) Su, C. -C.; Chiu, S. Y. *Polyhedron* **1996**, *15*, 2623.

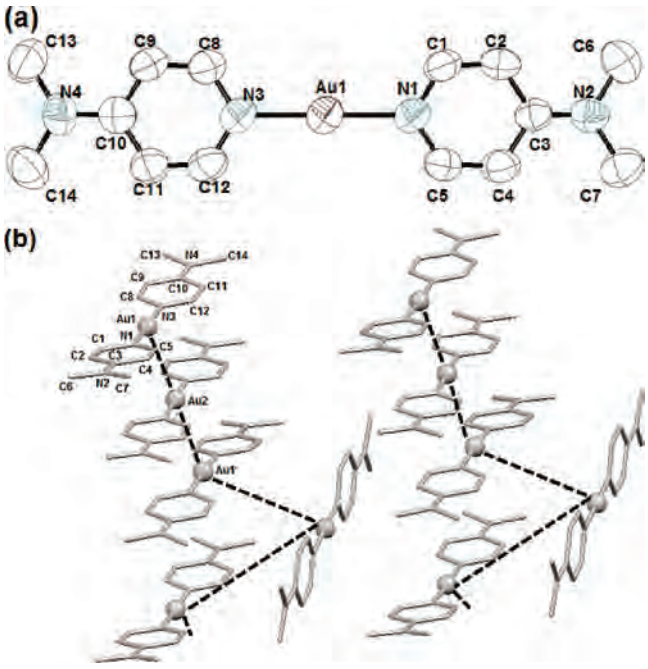

Figure 2. (a) ORTEP diagram of **Ib** (50% probability ellipsoids), (b) crystal packing diagram of $[Au(4\text{-dmapy})_2]^+$ with a [+ + +][+] pattern (the $[PF_6]^-$ ion and hydrogen atoms have been omitted for clarity). Selected bond lengths (Å) and angles (deg): Au(1)−N(1), 2.007(5); Au(1)−N(3), 2.012(5); N(1)−C(1), 1.336(7); N(1)−C(5), 1.354(7); N(3)−C(8), 1.348(7); N(3)−C(12), 1.340(7); N(2)−C(3), 1.349(7) ; N(4)−C(10), 1.329(7); N(1)−Au(1)−(N3), 177.10(17).

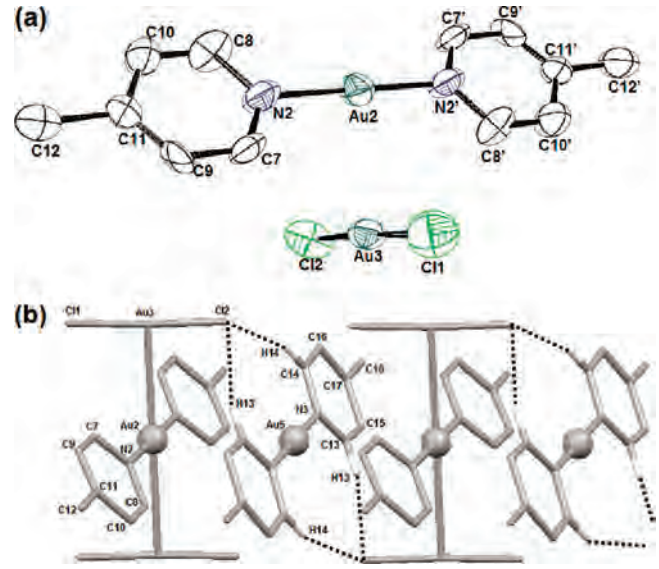

Figure 3. (a) ORTEP diagram of **IIa** (50% probability ellipsoids), (b) crystal packing diagram of **IIa** with a [− + −] [+] pattern (the hydrogen atoms have been omitted for clarity). Selected bond lengths (Å) and angles (deg): Au(2)−Au(3), 3.245(66); Au(2)−N(2), 2.068(48); Au(5)−N(3), 2.066(46); Au(3)−Cl(1), 2.282(12); Au(3)−Cl(2), 2.298(13); N(2)−C(7), 1.350(48); N(2)−C(8), 1.337(53); N(3)−C(13), 1.311(49); N(3)−C(14), 1.351(4); N(2)−Au(2)−N(2′), 180.00(9); N(3)−Au(5)−N(3′), 179.99(1); Cl(1)−Au(3)−Cl(2), 177.42(4); C(7)−N(2)−C(8), 117.72(2); C(13)−N(3)−C(14), 118.64(3).

+ +] and [+] arrangements. Within the [+ + +] unit, the cations are lined up parallel, in which a Au···Au contact of about 3.49 Å[1] and a pyridine−pyridine $\pi\cdots\pi$ interaction distance of about 3.50 Å are observed.[13] The isolated cation [+] sits between adjacent [+ + +] sets with a Au···Au distance of around 5.40 Å (Figure 2). A $[PF_6]^-$ ion bridges between the [+ + +] and [+] sets with C−H···F distances between 2.50 and 2.60 Å (Supporting Information).[14] Note that the crystal lattice also contained disordered CH_3CN solvent molecules.

$[Ag(4\text{-dmapy})_2][PF_6]$ was also prepared and crystallographically characterized (Supporting Information). It appears that a mere change of Au(I) by Ag(I) has tilted the delicate balance among "metalophilicity" and ring $\pi-\pi$ interactions. A different packing is assembled, in which the Ag centers line up perfectly with a separation of about 4.44 Å, with apparently no Ag···Ag interaction. This result would suggest that the Ag···Ag interaction is smaller than the Au···Au interaction.

$[Au(4\text{-pic})_2][AuCl_2]$ IIa. The crystal of **IIa** adopts a [− + −] [+] ion-pair packing (Figure 3) while the known $[Au(3\text{-pic})_2][AuCl_2]$ assumes a [+ − + − ···] arrangement and the reported complex of 2-picoline gives a neutral [Au(2-pic)Cl].[5d] In the set of [− + −], the $[Au(4\text{-pic})_2]^+$ cation is linked with two $[AuCl_2]^-$ anions through Au···Au distances of about 3.25 Å and 3.26 Å with linear Au(3)−Au(2)−Au(3′). Between the neighboring [− + −] and [+], the $[AuCl_2]^-$ anion forms two short Au−Cl···HC contacts with the ortho hydrogens of the pyridyl ring to become a 1-D array (Figure 4). The cations align into a perfect straight line with a Au···Au distance around 4.06 Å. These 1-D arrays turn into a 3-D network via the Au−Cl···HC hydrogen bonding (2.94 Å, 138°) utilizing the protons of the methyl substituents on pyridine (Supporting Information).

$[Au(4\text{-pic})_2][PF_6]$ IIb. Six $[Au(4\text{-pic})_2]^+$ cations are associated via aurophilic interactions to yield a [+ + + + + +] pattern as seen in Figure 4. The Au(3)−Au(2), Au(2)−Au(1), and Au(1)−Au(1′) lengths are about 3.32, 3.29, and 3.35 Å, respectively.[15] The 3.55–3.65 Å separation between the two nearest pyridyl rings suggests $\pi\cdots\pi$ interactions.[13] Short CH···F distances (2.5–2.6 Å) are generated between ring hydrogens and $[PF_6]^-$ (Supporting Information).[14] As a result, the Au skeleton is built of 1-D zigzagging Au chains in a unit of six Au's, in which the adjacent units are separated by 5.78Å. For comparison, the polymeric $[Au(3\text{-pic})_2]^+_n$ with $[SbF_6]^-$ counter-ions[5d] forms a 1-D straight chain with Au···Au contacts of 3.40 Å.

The crystal structure of $[Au(4\text{-phpy})_2][PF_6]$ **IIIb** was also determined (Supporting Information). Unlike the $[PF_6]^-$ complexes **Ib** and **IIb**, no Au···Au interactions were observed, likely because of the bulky 4-phpy ligands.

Molar Conductance. Molar conductivity (Λ_M) measurements were carried out at room temperature in CH_3CN with

(12) (a) Aullon, G.; Bellamy, D.; Brammer, L.; Bruton, E. A.; Orpen, A. G. *Chem. Commun.* **1998**, 653. (b) Bardaji, M.; Jones, P. G.; Laguna, A.; Villacampa, M. D.; Villaverde, N. *Dalton Trans.* **2003**, 4529. (c) Tzeng, B. C.; Yeh, H. T.; Wu, Y. L.; Kuo, J. H.; Lee, G. H.; Peng, S. M. *Inorg. Chem.* **2006**, *45*, 591. (d) Nishio, M. *CrystEngComm* **2004**, 130.
(13) Janiak, C. A. *Dalton Trans.* **2000**, 3885.
(14) (a) Grepioni, F.; Cojazzi, G.; Draper, S. M.; Scully, N.; Braga, D. *Organometallics* **1998**, *17*, 296. (b) Xu, C.; Anderson, G. K.; Brammer, L.; Braddock-Wilking, J.; Rath, N. P. *Organometallics* **1996**, *15*, 3972.
(15) Bondi, A. *J. Phys. Chem.* **1964**, *68*, 441.

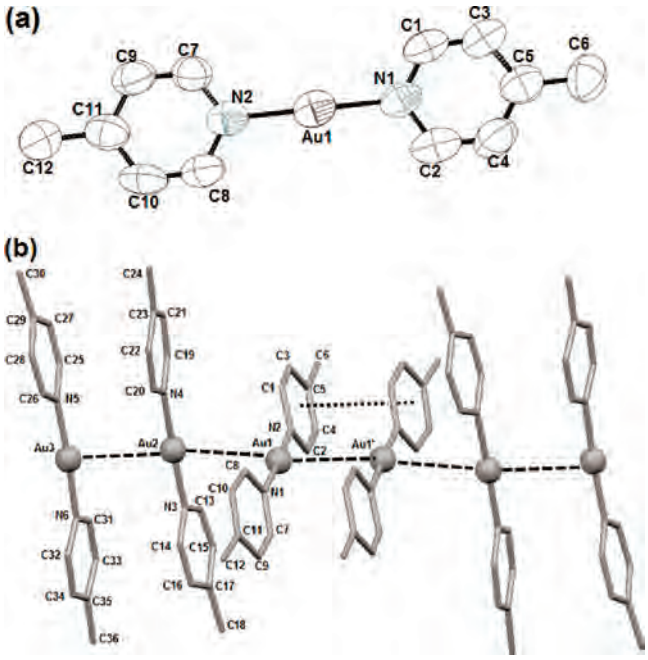

Figure 4. (a) ORTEP diagram of **IIb** (50% probability ellipsoids), (b) crystal packing diagram of $[Au(4\text{-pic})_2]^+$ with a [+ + + + + +] pattern (the $[PF_6]^-$ ion and hydrogen atoms have been omitted for clarity). Selected bond lengths (Å) and angles (deg): (Au(1)−Au(2), 3.2897(6); Au(1)−Au(1′) 3.3463(9); Au(2)−Au(3), 3.3242(6)); Au(1)−N(1), 2.011(11); Au(1)−N(2), 2.016(11); N(1)−C(1), 1.357(17); N(1)−C(2), 1.336(17); N(2)−C(7), 1.334(16);N(2)−C(8),1.340(16);N(1)−Au(1)−(N2),177.8(3);C(1)−N(1)−C(2), 117.6(13); C(8)−N(2)−C(7), 116.7(12); Au(2)−Au(1)−Au(1′), 166.47(3); Au(1)−Au(2)−Au(3), 166.42(2).

Table 1. Molar Conductivities of Au(I)−Py Complexes in CH_3CN

	complex	Λ_M, ohm^{-1} cm^2 mol^{-1}
Ia	$[Au(4\text{-dmapy})_2][AuCl_2]$	48
IIa	$[Au(4\text{-pic})_2][AuCl_2]$	74
IIIa	$[Au(4\text{-phpy})_2][AuCl_2]$	59
IVa	$[Au(4\text{-}^t\text{bupy})_2][AuCl_2]$	64
Ib	$[Au(4\text{-dmapy})_2][PF_6]$	205
IIb	$[Au(4\text{-pic})_2][PF_6]$	205
IIIb	$[Au(4\text{-phpy})_2][PF_6]$	200
IVb	$[Au(4\text{-}^t\text{bupy})_2][PF_6]$	176

concentrations of about 1.0×10^{-3} M, as given in Table 1. The Λ_M of **I**−**IVa** are in the range of 48–74 ohm^{-1} cm^2 mol^{-1}, smaller than the 120–160 ohm^{-1} cm^2 mol^{-1} expected for 1:1 electrolytes as reported in the literature.[16] This is likely due to (i) ion-pair formation promoted by the Au···Au interactions and (ii) the possible equilibrium between [Au(py)Cl] and $[Au(py)_2][AuCl_2]$ in solution.[5a–d,17] Both behaviors might decrease the concentrations of ions as expected for a strong electrolyte.

On the other hand, the Λ_M values of 176–205 ohm^{-1} cm^2 mol^{-1} found for complexes **I**−**IVb** are higher than those for 1:1 electrolytes but lower than the 220–300 ohm^{-1} cm^2 mol^{-1} expected for 1:2 electrolytes.[16] With a large noncoordinating $[PF_6]^-$ anion, **I**−**IVb** are expected to behave as strong electrolytes. Typically for a strong 1:1 electrolyte in solution

(16) Geary, W. J. *Coord. Chem. Rev.* **1971**, *7*, 81.
(17) (a) Guy, J. J.; Jones, P. G.; Mays, M. J.; Sheldrick, G. M. *J. Chem. Soc., Dalton Trans.* **1977**, 8. (d) Ahrland, S.; Noren, B.; Oskarsson, A. *Inorg. Chem.* **1985**, *24*, 1330. (e) Lock, C. J. L.; Wang, Z. *Acta Crystallogr.* **1993**, *C49*, 1330. (h) Ahrens, B.; Jones, P. G.; Fischer, A. K. *Eur. J. Inorg. Chem,* **1999**, 1103.

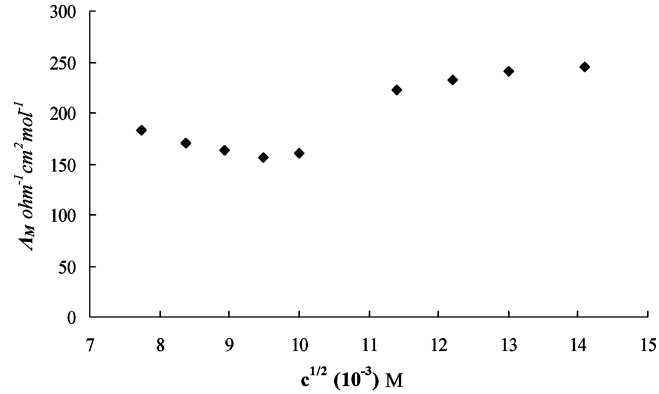

Figure 5. Molar conductivity of a CH_3CN solution of **Ib**, as a function of the square root of the concentration.

at a concentration of less than 2.0×10^{-3} M, the Λ_M vs $c^{1/2}$ should be linear and, owing to the interionic force, the Λ_M decrease slightly with increasing concentration. The plot of Λ_M vs $c^{1/2}$ for **Ib** in Figure 5 shows a linear decrease in Λ_M with increasing concentration in the range of 6.0×10^{-5}−9.0×10^{-5} M, as expected for a 1:1 strong electrolyte. However, for a further elevation from 1.0×10^{-4} to 2.0×10^{-4} M, instead of a continuing decrease in Λ_M, an unexpected increase is observed. The phenomenon argues against a simple 1:1 electrolyte and favors possible formation of an electrolyte higher than 1:1. As stated earlier, in the solid state, molecular cations of **Ib** aggregate via aurophilicity. In solution, this interaction may also occur such that cations of **Ib** associate to produce the 1:2 electrolyte $[(Au(4\text{-dmapy})_2)_2][PF_6]_2$. Aggregation of cationic Au(I) in solution has been reported.[3f,g] For an equilibrium between the monocation and dication (eq 1), a higher **Ib** concentration will favor the formation of more dicationic species. Present data indicate that at a concentration as low as 1.0×10^{-4} M, a substantial amount of dicationic species is formed. Further study of the equilibrium between the monocation and dication by UV–vis spectrometry are reported in the section that follows.

$$2[AuPy_2][PF_6] \rightleftharpoons [(AuPy_2)_2][PF_6]_2$$
$$\text{monocationic} \qquad \text{dicationic}$$
$$K = [\text{dication}]/[\text{monocation}]^2 \qquad (1)$$

Photophysical Properties. Absorption Spectra. In solution, the electronic absorption spectra of all complexes exhibit a high energy (HE) band and a low energy (LE) band in the UV region. The relative intensity of these two bands is temperature and concentration dependent. The temperature dependent UV–vis absorption spectrum of **Ib** is shown in Figure 6a. At 40 °C, a HE band appears at 257 nm and a LE band of slightly higher intensity at 292 nm. As the temperature is lowered to 35 °C, 32 °C, 28 °C, and then 23 °C, a significant increase in the intensity of the LE band and the presence of an isosbestic point are observed. The latter indicates that two species are in equilibrium. As stated earlier, the two equilibrium species in solution are likely $[AuPy_2]^+$ and $[(AuPy_2)_2]^{2+}$. We propose that the HE band can be attributed to mononuclear $[AuPy_2]^+$ while the LE band

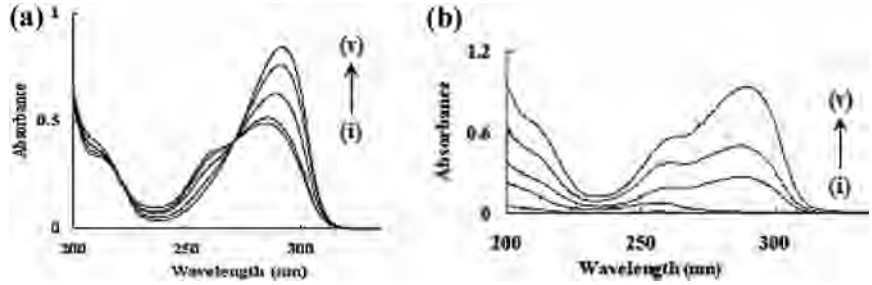

Figure 6. (a) Temperature dependent absorption spectrum of **Ib**: (i) 40 °C, (ii) 35 °C, (iii) 32 °C, (iv) 28 °C, (v) 23 °C. (b) Concentration dependent absorption spectra of **Ib**: (i) 6.60×10^{-6} M, (ii) 1.74×10^{-5} M, (iii) 1.09×10^{-4} M, (iv) 1.90×10^{-4} M, (v) 2.72×10^{-4} M.

Table 2. Emission Spectral Data for Au(I)−Py Complexes

	compound	excitation	emission λ_{max} (fine-structure), nm	ligand emission
Ia	$[Au(4\text{-dampy})_2][AuCl_2]$	360	~499 (439, 468, 499, 534) 610 (sh)	335
IIa	$[Au(4\text{-pic})_2][AuCl_2]$	360	~495 (462, 495, 530)	380
IIIa	$[Au(4\text{-phpy})_2][AuCl_2]$	360	~500 (438, 468, 500, 536)	470
IVa	$[Au(4\text{-}t\text{-butylpy})_2][AuCl_2]$	320	~446 (446, 476, 510)	385
Ib	$[Au(4\text{-dampy})_2][PF_6]$	360	405, 520 (sh)	
IIb	$[Au(4\text{-pic})_2][PF_6]$	360	430	
IIIb	$[Au(4\text{-phpy})_2][PF_6]$	360	~500 (437, 466, 500, 538)	
IVb	$[Au(4\text{-}t\text{-butylpy})_2][PF_6]$	320	442, 472, 505 (sh)	

results from the dinuclear $[(AuPy_2)_2]^{2+}$, as observed in other systems.[3f,g]

Figure 6b gives the concentration dependent absorption spectra of **Ib**. An elevation of concentration from 6.60×10^{-6} to 2.72×10^{-4} M results in a drastic growth in the intensity of the LE band compared with the HE band. Notably, the LE absorption is not observed in the two most dilute solutions of 6.60×10^{-6} and 1.74×10^{-5} M. The nonlinear growth in the intensity of the absorption band upon increasing the concentration is consistent with the occurrence of molecular aggregation. Assuming an equilibrium between mononuclear and dinuclear species, eq 2 can be used to estimate the equilibrium parameters,

$$[M]_o/A_2 = 1/(\varepsilon_2 Kb)^{1/2} + 2A_2^{1/2}/b \qquad (2)$$

where $[M]_o$ is the initial concentration of the mononuclear species, K is the equilibrium constant, b is the cell path length, A_2 is the absorbance of the dinuclear species, and ε_2 is the extinction coefficient of the dinuclear species. The plot of $[M]_o/A_2^{1/2}$ versus $A_2^{1/2}$ for **Ib** is a straight line, supporting the proposed equilibrium, in which ε_2 is estimated to be 7.12×10^4 M^{-1} cm^{-1} with equilibrium constant $K = 8.0 \times 10^3$. A plot of log K versus $1/T$ yields the association enthalpy and entropy of -14 ± 5 kcal mol^{-1} and -10 ± 8 cal K^{-1} mol^{-1} from the slope and intercept, respectively. It has been reported that the Au···Au interaction is typically in the range of 6–11 kcal/mol;[3] the slightly higher enthalpy observed in this work suggests that other interactions such as ring $\pi-\pi$ interactions may also contribute to the associative process; the negative entropy is consistent with an associative process. The magnitudes of equilibrium constants and thermodynamic parameters derived for **Ib** are in line with aurophilic aggregation, as stated by Schmidbaur.[18]

Density functional B3LYP/LanL2DZ calculations[9] were performed for mononuclear $[Au(4\text{-dmapy})_2]^+$ and dinuclear $[(Au(4\text{-dmapy})_2)_2]^{2+}$, for which we assumed the arrangements as in the crystal of the **Ib** compound. The computations predict a smaller highest occupied molecular orbital (HOMO)–lowest unoccupied molecular orbital (LUMO) gap for the dinuclear species than the one in the mononuclear species. This appears to be consistent with the assignment of LE and HE bands in the absorption spectra with contributions from the dinuclear and mononuclear species, respectively, assuming that the absorption of a photon results in the promotion of an electron from the HOMO to the LUMO. An isolated $[(Au(4\text{-dmapy})_2)_2]^{2+}$ is not stable, where the monomers prefer to stay apart in vacuum. However, two $[PF_6]^-$ anions can stabilize the dicationic $[(Au(4\text{-dmapy})_2)_2]^{2+}$, as the present level of theory indicates. Thus, it is reasonable to anticipate that at low enough concentrations the solution would be too dilute to sustain even the simplest aggregated species, $[(Au(4\text{-dmapy})_2)_2]^{2+}$. The scenario seems to be demonstrated nicely at the concentrations of 6.60×10^{-6} M and 1.74×10^{-5} M in Figure 6b, where the LE band is practically nonexistent.

Similarly, the electronic absorption spectra of **Ia** in solution are also concentration and temperature dependent (Supporting Information). At a concentration as low as 7.16×10^{-6} M, equally weak HE (261 nm) and LE (283 nm) bands were observed. Upon increasing concentration to 3.80×10^{-5} M, the LE band intensity increases more substantially than that of the HE band. However, unlike **Ib**, no isosbestic point is observed upon changing the temperature between 40 and 22 °C. This result indicates that the presence of more than two species, such as the neutral form, [+][−], [+ −], [+ − +

(18) (a) Mathieson, T.; Schier, A.; Schmidbaur, H. *Dalton Trans.* **2001**, 1196. (b) Hunks, W. J.; Jennings, M. C.; Puddephatt, R. J. *Inorg. Chem.* **2000**, *39*, 2699. (c) Ho, S. Y.; Cheng, E. C. C.; Tiekink, E. R. T.; Yam, V. W. W. *Inorg. Chem.* **2006**, *45*, 8165. (d) White-Morris, R. L.; Olmstead, M. M.; Attar, S.; Balch, A. L. *Inorg. Chem.* **2005**, *44*, 5021. (e) Su, H. C.; Fadhel, O.; Yang, C. J.; Cho, T. Y.; Fave, C.; Hissler, M.; Wu, C. C.; Reau, R. *J. Am. Chem. Soc.* **2006**, *128*, 983. (f) Siemeling, U.; Rother, D.; Bruhn, C.; Fink, H.; Weidner, T.; Trager, F.; Rothenberger, A.; Fenske, D.; Priebe, A.; Maurer, J.; Winter, R. *J. Am. Chem. Soc.* **2005**, *127*, 1102. (g) Chao, H. Y.; Lu, W.; Li, Y.; Chan, M. C. W.; Che, C. M.; Cheung, K. K.; Zhu, N. *J. Am. Chem. Soc.* **2002**, *124*, 14696. (h) White-Morris, R. L.; Olmstead, M. M.; Jiang, F.; Tinti, D. S.; Balch, A. L. *J. Am. Chem. Soc.* **2002**, *124*, 2327.

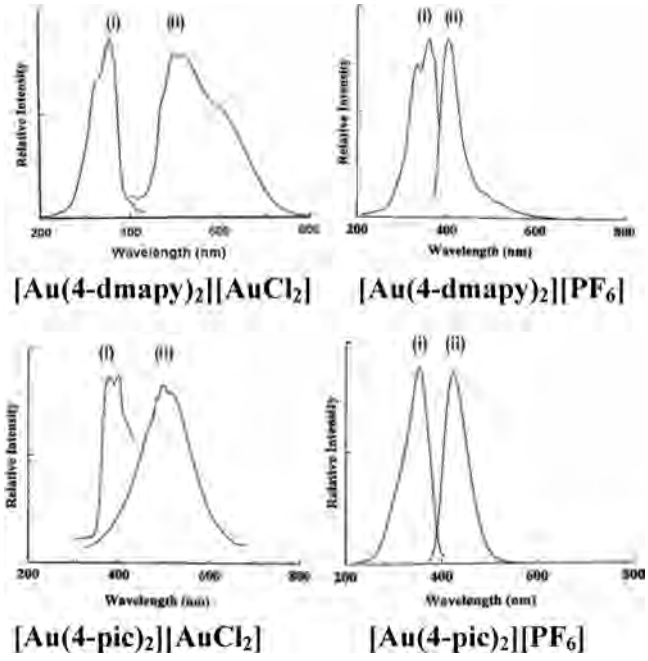

Figure 7. Emission spectra of crystalline **Ia**, **Ib**, **IIa**, and **IIb**; (i) excitation, (ii) emission.

−], [− + + −], or others, with or without Au···Au interactions, is likely.

As indicated by the B3LYP/LanL2DZ calculations, in contrast to the dinuclear $[(Au(4\text{-dmapy})_2)_2]^{2+}$, the **Ia** ion-pair could exist comfortably and, in fact, is energetically more stable than two separated ions. The extent of the concentration dependence is not as prominent in the absorption spectra of the **Ia** solution as in the **Ib** counterpart. That the LE band lingers even at the lowest concentration measured, 7.16×10^{-6} M, could be attributed to the **Ia** ion-pair, that is, [+ −].

Emission Spectra. Compounds **I**−**IV** are luminescent in the solid state at room temperature with long life times in the tens of microseconds. On the other hand, $[Ag(4\text{-dmapy})_2][PF_6]$, an analogous silver compound, is nonluminescent. Features of solid-state emission spectra of **I**−**IV** at room temperature are summarized in Table 2. As seen in Figure 7, **Ia** and **IIa** both show a structured band at $\lambda_{max} =$ 500 nm. In **Ia**, the structured band is followed by a broad shoulder at 610 nm. Their $[PF_6]^-$ counterparts, **Ib** and **IIb**, give an intense and featureless band of λ_{max} at 405 and 430 nm, respectively, with the former tailed by several very weak peaks.

Figure 8 discloses that the HOMO of ion-pair **Ia** is the HOMO of the $[AuCl_2]^-$ species, while the LUMO is practically the LUMO of the $[Au(4\text{-dmapy})_2]^+$ entity. The **Ia** HOMO is a heavily hybridized orbital involving the metal and Cl^-; the LUMO on the other hand, predominately belongs to the 4-dmapy ligand, with a minor contribution from the metal. On the basis of the theoretical prediction at the present level, the observed phosphorescence may be pictured as a consequence of the transition of an electron from the $[Au(4\text{-dmapy})_2]^+$ to its counterion $[AuCl_2]^-$. Thus, the spectra is expected to be ligand (4-dmapy) related, which is in line with the observation from Figure 7 that the vibronic spacings are in the range of 1400–1600 cm^{-1}, in good agreement with the skeletal vibration frequencies (C═C and C═N) of the pyridyl rings.[19]

It would be tempting to assign the 610 nm shoulder to the Au···Au interaction.[20] However, the HOMO and LUMO of the **Ia** molecule involve only a single Au atom, which implies that neither HOMO nor LUMO exhibits the aurophilicity. The highest occupied molecular orbital with evidence of a Au···Au interaction is buried down in the third HOMO (THOMO), while the LUMO with some sign of aurophilicity does not appear until the sixth LUMO. This signifies that for the **Ia** compound, aurophilicity would not influence the spectra directly, even though it appears in the crystal structure obtained in the current work. That is, the present level of calculation does not support that the emission band is the result of aurophilicity.

The situation persists for system of **IIa**. Namely, the HOMO of ion-pair **IIa** is again the HOMO of $AuCl_2^-$, and the LUMO of **IIa** is the $[Au(4\text{-pic})_2]^+$ LUMO. The absence of a Au···Au interaction in both HOMO and LUMO is an indication that aurophilicity also does not play a vital role in the spectra of the **IIa** compound.

In the systems with $[PF_6]^-$ as counteranion, the circumstances differ, however. Distinct from the substantial hybridization between the orbitals of the $[AuCl_2]^-$ anion and those of the Au(I)−Py complex in **Ia** and **IIa**, the calculations show that $[PF_6]^-$ plays a rather passive role and does not participate in forming molecular orbitals with energies in the proximity of the HOMO and LUMO of the systems. As illustrated in Figure 9, for the **IIb** compound, the HOMO and LUMO of $[(Au(4\text{-pic})_2)_2]^{2+}$ are simply composed of the HOMO and LUMO of two $[Au(4\text{-pic})_2]^+$, respectively. While the $[(Au(4\text{-pic})_2)_2]^{2+}$ LUMO is associated with 4-pic, it can be easily seen that the HOMO almost entirely stems from two Au atoms, thus indicating that the Au···Au interaction plays a role. In contrast to the **IIa** compound, the property of aurophilicity could deeply affect the spectra of **IIb** through the ground-state HOMO.

Ib bears a resemblance to **IIb** in the nature of its HOMO and LUMO. The ground state $[(Au(4\text{-dmapy})_2)_2]^{2+}$ HOMO arises from the HOMOs of two $[Au(4\text{-dmapy})_2]^+$/$[Au(4\text{-dmapy})_2]^+$ and likewise its LUMO, the LUMOs of monomers. In the HOMO of $[(Au(4\text{-dmapy})_2)_2]^{2+}$, considerable ligand character makes the Au···Au interaction less dominant than in $[(Au(4\text{-pic})_2)_2]^{2+}$; however, it nevertheless remains significant. Thus, one would anticipate that via the ground-state HOMO, aurophilicity could exert influence on the **Ib** spectra.

Interestingly, **Ia** and **IIa**, for which the HOMO and LUMO reveal no sign of the Au···Au interaction, both yield structured emission spectra, while the featureless spectra of **Ib** and **IIb** coincides with a Au···Au interaction embedded HOMO. It would be logical to correlate the striking feature-

(19) Tzeng, B. C.; Liao, J. H.; Lee, G. H.; Peng, S. M. *Inorg. Chim. Acta* **2004**, *357*, 1405.
(20) (a) Wang, H. M. J.; Vasam, C. S.; Tsai, T. Y. R.; Chen, S. H.; Chang, A. H. H.; Lin, I. J. B. *Organometallics* **2005**, *24*, 486. (b) Wang, H. M. J.; Chen, C. Y. L.; Lin, I. J. B. *Organometallics* **1999**, *18*, 1216.

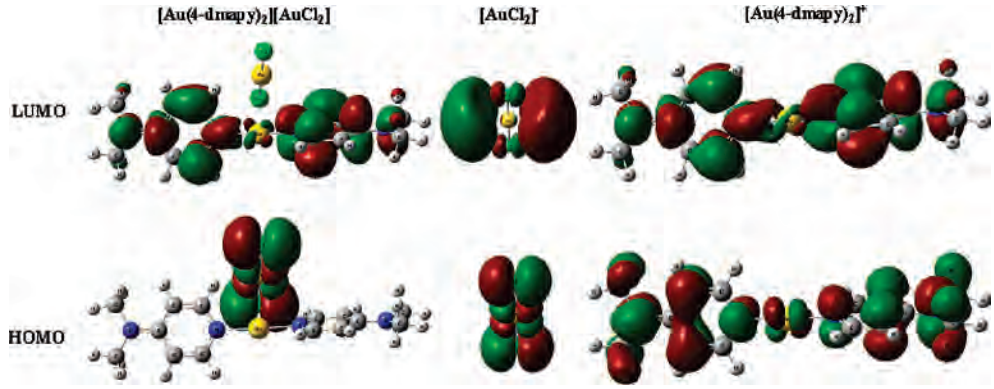

Figure 8. B3LYP/LanL2DZ molecular orbitals of the **Ia** ion pair, $[AuCl_2]^-$, and $[Au(4\text{-dmapy})_2]^+$.

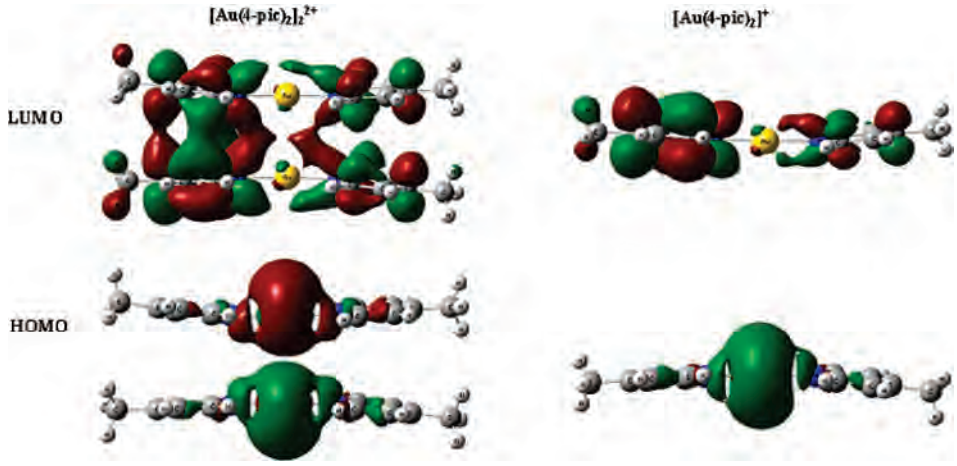

Figure 9. B3LYP/LanL2DZ molecular orbitals of $[(Au(4\text{-pic})_2)_2]^{2+}$and $[Au(4\text{-pic})_2]^+$.

less emissions of **Ib** and **IIb** to a Au···Au interaction in their HOMOs.

Catalysis. The richness of homogeneous and heterogeneous gold catalysis has only been realized quite recently. The use of Au(I) complexes as potential catalysts for Suzuki cross-coupling reactions was studied by Corma et al.,[21] in which the electronic effects of ligands were examined. Our preliminary results employing one of the Au(I)−Pys in catalyzing the Suzuki cross-coupling reaction are presented as follows.

$[Au(4\text{-dmapy})_2][AuCl_2]$ Ia. This compound was utilized as a catalyst in the coupling of *p*-bromo toluene with phenylboronic acid. Reactions were carried out at 130 and 25 °C (room temperature, rt) in DMF under both aerobic and N_2 atmospheric conditions with base K_2CO_3 (Scheme 2). As tabulated in Table 3, under aerobic condition the cross-coupling product, *P*-phenyl toluene, was generated in a GC yield of 90% at 130 °C (6 h) and 52% at rt (22 h). On the other hand, under a N_2 atmosphere and a prolonged reaction time of 22 h, *P*-phenyl toluene was obtained with 95% yield at 130 °C and a mere about 5% yield at rt. Apparently, reactions under air at high temperature gave a better cross-coupling product yield with catalyst **Ia**. As far as we know, no Au(I) catalyst has been reported to activate the cross-coupling between phenyl bromide and phenylboronic acid. However, the reaction was known to occur when the more reactive phenyl iodide was used (85% yield at 130 °C, 22 h).[21a] Corma et al.[21b,c] have attempted cross-coupling between phenyl bromide and boronic acid catalyzed with Au(I)/Au(III) complexes, which in turn yielded the homo-coupling product of boronic acid.

Scheme 2. Suzuki Cross-Coupling of *p*-Bromo Toluene with Phenylboronic Acid

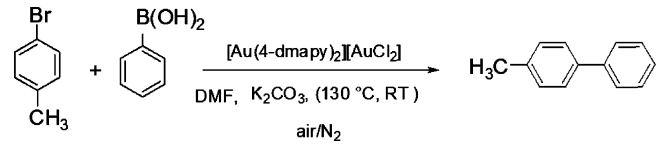

Table 3. Yields of Suzuki Cross-Coupling Reactions under Various Conditions

	130 °C		rt	
catalyst	air	N_2	air	N_2
Ia	90 (6)[a]	95(22)	52 (22)	<5 (22)

[a] Experimental: *p*-bromo toluene (0.30 mmol); phenylboronic acid (0.36 mmol); $[Au(4\text{-dmapy})_2][AuCl_2]$ (5% mol); K_2CO_3 (0.45 mmol); DMF (1 mL); GC yield; a: Yield % (h).

Conclusion

Eight Au(I) complexes of 4-substituted pyridines were synthesized. With Au···Au interactions, the $[Au(4\text{-dmapy})_2][AuCl_2]$ and $[Au(4\text{-pic})_2][AuCl_2]$ complexes were

(21) (a) Corma, A.; Gutiérrez-Puebla, E.; Iglesias, M.; Monge, A.; Pérez-Ferreras, S.; Sánchez, F. *Adv. Synth. Catal.* **2006**, *348*, 1899. (b) González-Arellano, C.; Corma, A.; Iglesias, M.; Sánchez, F. *J. Catal.* **2006**, *238*, 497. (c) González-Arellano, C.; Corma, A.; Iglesias, M.; Sánchez, F. *Chem. Commun.* **2005**, 1990.

found to adopt [+ − + − •••] and [− + −] [+] crystal packing patterns, respectively. Their $[PF_6]^-$ counterparts, $[Au(4\text{-dmapy})_2][PF_6]$ and $[Au(4\text{-pic})_2][PF_6]$ complexes, however, crystallize in triset [+ + +] and hexa-set [+ + + + + +], respectively, also with the aid of aurophilic attractions. While the aurophilic interaction acts continuously along the infinite 1-D polymer of $[Au(4\text{-dmapy})_2][AuCl_2]$, it persists in discrete units of 3, 3, and 6 Au atoms for the crystals of $[Au(4\text{-pic})_2][AuCl_2]$, $[Au(4\text{-dmapy})_2][PF_6]$, and $[Au(4\text{-pic})_2][PF_6]$, respectively.

In solution, both the conductivity measurements and the absorption spectroscopic studies indicate molecular aggregation at high concentration. An equilibrium between the mononuclear $[AuPy_2]^+$ and the dinuclear $[(AuPy_2)_2]^{2+}$ is proposed for the $[PF_6]^-$ salts. The equilibrium constant and thermodynamic parameters of $[Au(4\text{-dmapy})_2][PF_6]$ are estimated based on the concentration-dependent and temperature-dependent absorption spectra, respectively. DFT calculations on the energetics of $[Au(4\text{-dmapy})_2]^+$, $[(Au(4\text{-dmapy})_2)_2]^{2+}$, and $[Au(4\text{-dmapy})_2][AuCl_2]$ ion-pair support the molecular aggregation in solution.

All the compounds are luminescent in the solid state. Analysis of the DFT derived molecular orbitals for ion-pairs, $[Au(4\text{-dmapy})_2][AuCl_2]$ and $[Au(4\text{-pic})_2][AuCl_2]$, mononuclear $[Au(4\text{-dmapy})_2]^+$, $[Au(4\text{-pic})_2]^+$, and $AuCl_2^-$, and dinuclear $[(Au(4\text{-dmapy})_2)_2]^{2+}$ and $[(Au(4\text{-pic})_2)_2]^{2+}$ indicates that the emissions of $[Au(4\text{-dmapy})_2][AuCl_2]$ and $[Au(4\text{-pic})_2][AuCl_2]$ are mainly ligand in nature, whereas those from $[Au(4\text{-dmapy})_2][PF_6]$ and $[Au(4\text{-pic})_2][PF_6]$ crystals involve aurophilic interactions.

Preliminary results show that contrary to the known Au(I) catalysts, **Ia** is effective in catalyzing the cross-coupling of aryl bromides with phenylboronic acid. While the use of Au compounds as catalysts is still in infancy, our work could encourage further efforts on the utilization of Au(I) complexes in catalysis.

Acknowledgment. The authors wish to thank National Science Council of Taiwan for the financial support (NSC 95-2113-M-259-012, NSC 95-2113-M-259-005), Prof. F. E. Budenholzer at Fu Jen Catholic University for the proof reading of the manuscript, and National Center for High-performance Computer of Taiwan for computer resources.

Supporting Information Available: Figures, tables, and crystallographic data for the compounds (PDF). This material is available free of charge via the Internet at http://pubs.acs.org.

IC701872F